Performance of a vapor-fed PBI-based Direct Methanol Fuel Cell

Justo Lobato, Pablo Cañizares, Manuel A. Rodrigo, José J. Linares, Rubén López-Vizcaíno*

Chemical Engineering Department, University of Castilla-La Mancha, Campus Universitario s/n. 13004, Ciudad Real, Spain.

Abstract

A high temperature vapor-fed direct methanol fuel cell (DMFC) has been implemented using H_3PO_4-doped polybenzimidazole (PBI) as the electrolyte. The influence of the cell temperature, the methanol concentration and the oxygen partial pressure has been studied. This investigation included the evaluation of the cell performance, each electrode potential and crossover current. A lifetime test for 10 days was intermittently carried out in order to assess the stability of the cell response. Increases in the temperature notably enhanced the performance of the cell, although the methanol crossover also increased. The methanol concentration was found to have an optimum value, since a low amount of methanol led to mass transfer limitations and a large amount promoted the crossover and limited the availability of water for methanol oxidation. An increase in the oxygen partial pressure markedly improved the cell response. The higher comburent availability and reduced methanol crossover effect explain this behavior. The study of the combined effect of the oxygen partial pressure and methanol concentration confirmed this effect. The preliminary durability results showed quite stable performance for the cell at a constant current density of

100 mA cm^{-2}. Finally, a comparison between PBI and the traditional DMFC membrane (Nafion®) was carried out. This comparison showed the PBI-based cell to be a good candidate for DMFC.

Keywords: DMFC, PBI, high temperature, methanol vapor, methanol crossover

To whom correspondence should be addressed: justo.lobato@uclm.es

1. Introduction

Direct methanol fuel cells (DMFCs) show some advantages over hydrogen-fed polymeric electrolyte membrane fuel cells (PEMFCs). Methanol as a fuel has a high power density per mass unit (6 kWh/kg) [a value comparable to that of gasoline (10-11 kWh/kg)] and can be handled, stored and transported easily[1]. However, the present DMFC technology has two major limitations: (i) poor oxidation kinetics of the fuel and (ii) the permeation of methanol into the cathode, which depolarizes it and lowers the fuel and comburent utilisation[1-5]. These factors markedly reduce the cell performance and, as a consequence, the efficiency of the system, slowing the full development of the technology. Three main approaches have been proposed to overcome these problems: (i) a more active catalyst for methanol oxidation[6-9], (ii) methanol-tolerant cathode catalysts[10-12], and (iii) membranes with a lower methanol permeability[2-4,13-16].

One approach that, to some extent, combines the three previous suggestions is an increase in the operating temperature, with the cell fed with a mixture of methanol and water in the vapor phase. The positive aspects of this type of system are collected in the literature[5,17-21]. According to Hogarth et al.[17,18] and Scott et al.[5], some of the

advantages include: (i) no requirement for methanol dilution, thus making it possible to operate with the same methanol solution for long periods if the fuel exhaust is recycled, (ii) the mass transfer and electrode kinetics are enhanced, (iii) the possibility of higher methanol fuel conversions, (iv) the absence of gas bubble formation, (v) use of the existing gas diffusion electrodes and (vi) a higher tolerance of the cathode to methanol crossover. These advantages, in conjunction with a low methanol permeable polymeric electrolyte, represent a very interesting option for DMFC.

A suitable material for the aforementioned conditions is polybenzimidazole, PBI. This material has interesting conductivity values above 120 ºC when doped with H_3PO_4[22-24] and has a low methanol permeation level[24-27]. The relatively weak bonding between H_3PO_4 and PBI (only 2 of the typically used 6–7 molecules of acid per PBI repeating unit are chemically bonded to the polymer backbone[28,29]) makes it necessary to operate in the vapor state in order to avoid washing-out of the H_3PO_4 by the water/methanol mixture. The dense, nonporous structure of the phosphoric acid-doped PBI membranes explains the low methanol permeability[26]. Furthermore, the particular mechanism of proton transport (*Grotthus mechanism*) means that the electro-osmotic drag coefficient of methanol and water (similar properties) is near to 0[30]. This is not the case with Nafion®, the structure of which has interconnected hydrophilic domains that make it quite permeable to water and methanol[31]. A more detrimental factor is the proton movement, which occurs by the so-called "*vehicle mechanism"*, which involves the protons travelling along the membrane with water (or methanol) molecules (electro-osmotic drag coefficient of 2–3[31,32]). As a consequence, in a Nafion®-based DMFC, unacceptable amounts of methanol cross the membrane from the anode to the cathode. Furthermore, the requirement of water for the movement of

protons does not allow operation of the cell at temperatures above 100 ºC at atmospheric pressure and this makes it more difficult to maintain the water balance.

PBI has previously been used for DMFC. In 1995 Wainright et al.[25] presented the first results for a PBI-based fuel cell with a DMFC system. They used PtRu and Pt black electrocatalysts for the anode and cathode, respectively, with loadings of 4 mg cm^{-2}, operating at 200 ºC and feeding the cell with a water/methanol molar ratio of 4:1. The PBI membrane used was 100 µm thick and had a doping level of 5 molecules of acid per PBI repeating unit. The power peak of the cell was over 100 mW cm^{-2} for current densities between 250 and 500 mA cm^{-2}. In 1996, Wang et al.[33] published a more extensive study in which the influence of several operating parameters was analyzed; these included temperature, water/methanol ratio, catalyst loading and oxygen partial pressure. The performance of each electrode was analyzed in detail. In the same year, Wang et al.[26] measured the methanol crossover and electro-osmotic drag in a PBI-based DMFC by a real-time mass spectrometric study. Lin et al.[34] in 1997 determined the product distribution of the exhaust anode gas of the cell depending on the temperature and the gas composition. Other studies were subsequently devoted to the search for methanol-tolerant cathode catalysts[11,35] and to alternative fuels (formic acid, ethanol, 1-propanol, 2-propanol, trimethoxymethane, methyl formate)[36-38]. PBI has also been used in the formation of composite membranes. Hobson et al.[39] proposed the use of a mixture of Nafion® and PBI. Wycisk et al.[40] and Ainla and Brandell[41] continued this line of investigation with very promising results and reduced methanol crossover in comparison to that obtained in pure Nafion® systems. Manea and Mulder[13] prepared a blend of sulfonated polysulfone and PBI with a low methanol permeation. Silva et al.[2,42] proposed an alternative involving the use of sulfonated

poly(etheretherketone) mixed with zirconium phosphate and PBI. They found an optimum ratio for the components to give acceptable levels of proton conductivity and methanol crossover. The most recent and outstanding advance in the field of PBI-based DMFC came with the commercialization of Celtec-V membranes for DMFC. These are based on a blend of PBI and polyvinylphosphonic acid (PVPA)[43]. Celtec-V is based on the idea of immobilizing an acid within the structure of PBI in order to avoid the undesirable washing-out phenomenon of the acid electrolyte[43,44] and allowing the use of liquid fuels. Very encouraging results were presented by Gubler et al.[44], although some issues need to be improved, such as the conductivity, cathode performance at high current density, and performance-degradation during durability tests.

The work described here concerns an investigation into the field of vapor-fed PBI-based DMFCs, showing the performance of this system under different operating conditions. The study also involved a preliminary lifetime test and comparison of the results with those of traditionally used Nafion® membranes for DMFC in order to establish a relative ranking of this non-fluorinated membrane.

2. Experimental

2.1. Membrane electrode assembly preparation

Membrane electrode assemblies (MEA) were prepared according to the following procedures.

(i) PBI-based MEA: A mixture of the catalyst [40% Pt and 20% Ru on Vulcan XC-72R Carbon, ca. atomic ratio 1:1 (Johnson Matthey) for the PtRu-based anode, and

60% Pt on Vulcan XC-72R Carbon (Johnson Matthey) for the Pt-based cathode], PBI solution (3.92% wt in *N,N'*-dimethylacetamide, DMAc) and DMAc (99%, Panreac) was sprayed onto of a carbon gas diffusion layer (Toray Graphite Paper, TGPH-120, 40% wet-proofed, E-TEK Inc.) by N_2-brushing until platinum and PBI loadings of 1 mg/cm^2 and 0.5 mg/cm^2, respectively, were achieved for the anode. The same procedure was used for the cathode. In this case, the PBI loading was 0.33 mg/cm^2. After depositing the catalyst layers, the electrodes were dried and cured at 190 ºC for 2 hours inside a N_2-ventilated oven. All the electrodes were subsequently soaked in 1 M phosphoric acid, on the basis of a H_3PO_4/PBI weight ratio of 6, and left to impregnate overnight. The required piece of membrane was taken from a bath of 75% wt. H_3PO_4 (doping level of 6.7). The procedure for the production of the polymer and the membranes is described elsewhere[24,45]. The active area of the electrodes was 4.65 cm^2. MEAs assembled by this procedure were stored in closed bags until further use.

(ii) Nafion®-based MEA: A mixture of PtRu/C catalyst (40% Pt and 20% Ru on Vulcan XC-72R Carbon, ca. atomic ratio 1:1, Johnson Matthey), Nafion® emulsion (5% wt in a mixture of aliphatic alcohols, Sigma Aldrich) and isopropyl alcohol (+99.5%, Panreac) was sprayed onto a carbon gas diffusion layer (Toray Graphite Paper, TGPH-120, 40% wet-proofed, E-TEK Inc.) by air-brushing until a platinum loading of 1 mg/cm^2 was achieved for the anode. The same procedure was used for the cathode, but a Pt/C catalyst (60% Pt on Vulcan XC-72R Carbon, Johnson Matthey) was used. Once the catalyst layers had been deposited, an additional amount of Nafion (1 mg/cm^2) was added in order to improve the adhesion of the electrodes to the membrane and to reduce the contact resistance between them. The electrodes (4.65 cm^2) were assembled with the membrane (Nafion® 117, 178 μm thick, DuPont Inc.)

by hot-pressing at 133 ºC and 100 Kg/cm^2 for 3 minutes. MEAs assembled by this procedure were stored in closed bags until further use.

2.2. Experimental set-up

There are two basic options for the implementation of a vapor-fed system[5,18]. One of these involves the use of an inert carrier gas such as nitrogen or argon. The disadvantage of this method is the diluting effect of the inert gas and the difficulty in controlling the supply of methanol. The other option consists of a sudden vaporization (flash) of the liquid mixture, which overcomes the aforementioned limitations. In order to achieve this goal, an experimental set-up was implemented and this is represented in Figure 1(a). The desired amount of methanol/water was pumped with a peristaltic pump (Percom-I, JP Selecta, Spain). The liquid flow (approx. 2 ml/min) was regulated with a recirculation loop and measured by a flowmeter (Amidata, Spain) before being fed into a vaporizer. This unit consisted of a thick (diameter = 2 cm) stainless steel tube with a heating cable wrapped around it. The steam generated in this way entered the anodic compartment of the DMFC. A fuel recovery system was employed. The exhaust vapor exited the cell through a heated silicone line and was returned to the original container equipped with a water-cooled condensing coil. This arrangement enabled operation of the cell for many hours on a single reservoir of fuel. Oxygen (or air) was introduced directly into the cell without any pretreatment. The flow (500 ml min^{-1}) was controlled with the aid of a gas flowmeter (Amidata, Spain). A pressure regulator and a pressure gauge (Swagelok, Spain) were inserted in the outlet stream of the cathode in order to pressurize it.

The cell hardware consisted of two bipolar plates made of graphite impregnated with a phenolic resin (Sofacel S.A., Spain). Channels with a parallel geometry (1.5 mm wide, 1 mm deep with ridges 1 mm wide) were machined onto these plates. Two crossing holes were drilled in order to fit the cartridge heaters (150 W, Watlow Ibérica, S.L.U., Spain) to heat up the system. A thermocouple was also imbedded into the cathode in order to monitor and control the cell temperature at the desired cell value (Cal Controls, United Kingdom). Gold-plated metallic bolts were screwed into the blocks to allow electrical contact (Amidata, Spain). Two end plates were used for each monopolar plate. One of these plates was made of Victrex® PEEK™ (Amidata, Spain) and the second was made of stainless steel. The first plate was used to avoid any electrical shorting, and this material was chosen as it possesses quite high thermal resistance (maximum operating temperature 180–220 ºC[46]). The stainless steel plate provided rigidity to the system. Four holes were drilled in this plate in order to locate the screws that clamped the cell. Swagelok® fittings were used for the connections of the fuel and comburent lines. A picture of the cell is shown in Figure 1(b). The MEA was placed between the graphite plates using compressible 0.5 mm thick Teflon (Gore-Tex GR, Gore Tex) as gaskets.

Figure 1

The system described above is suitable for the vapor-feed system. The measurements with the Nafion®-based MEA were performed with the fuel feed in the liquid state. The same system was used for this operation, with the exception of the use of the heating cable. The same flows for the fuel and the comburent were used.

2.3. Electrochemical measurements

Cell measurements were performed galvanostatically with the current fixed at the desired value. Prior to measurement a short time was allowed to elapse for a stable potential value to be reached, which usually took around 5 minutes. Current values were fixed by a power supply (DC Power Supply ES030-5, Delta Elektronika BV, The Netherlands). Measurements were repeated until reproducible polarization curves were obtained. This procedure is called cell conditioning and usually lasts for several days.

In order to measure the anode potential, a nitrogen flow was passed through the cathode. In this way, hydrogen evolves according to the following reaction:

$$2H^+ + 2e^- \rightarrow H_2 \uparrow \quad (1)$$

This allows the cathode to be used as a dynamic hydrogen reference electrode (DHE)[47], assuming that changes in its potential are negligible over the range of current densities used. Ideally, the anode potential should be iR-free reported. However, our DMFC test station did not allow the ohmic resistance to be measured. In an effort to estimate this parameter, we propose to use the semi-empirical model proposed by Argyropoulos et al.[48]. Thus, the anodic performance was fitted to the following expression.

$$E_a = E_{0a} + b_a \cdot \log i + i \cdot R - C_1 \ln(1 - C_2 \cdot i) \quad (2)$$

The parameter E_a (mV) is the anode potential, E_{0a} (mV) is the open circuit potential of the anode, b_a (mV) is the Tafel slope of the methanol oxidation, i (A cm^{-2}) the current

density, R (Ω cm^2) is the ohmic resistance of the system, C_1 (mV) is related to reaction kinetics and C_2 (cm^2 A^{-1}) to mass transfer limitations. The anode potential curves were corrected with the estimated R value. The cathode potential was calculated by the addition of the experimental anode potential to the cell value. Assuming that the ohmic resistance does not change significantly during the measurements of the anode and cell potential, both including the iR-drop, the reported cathode potentials can be considered to be the real ones (iR-free).

Limiting methanol permeation currents through the membrane in the real fuel cell were measured voltammetrically[32]. This method consists of inverting the cell polarity with respect to that used in the fuel cell normal mode, so that a limiting current density is measured due to the transport-controlled methanol oxidation at the former cathode (now the anode) of the fuel cell fed with inert N_2. In the former anode (now the cathode) hydrogen evolution takes place, serving as a counter and reference electrode. The system is represented in Figure 2. The actual crossover current is somewhat larger than the measured limiting current density. This is due to the counter methanol flux associated with the electro-osmotic drag of fluid by the protonic current corresponding to the limiting current[32]. Ren et al. developed an expression to obtain the crossover current ($J_{crossover}$, mA cm^{-2}) depending on the limiting current density (J_{lim}, mA cm^{-2}), the electro-osmotic drag coefficient (ε) and the methanol concentration (x_0 corresponding to the methanol molar fraction)[32].

$$\frac{J_{crossover}}{J_{lim}} = \frac{6 \cdot \varepsilon \cdot x_0}{\ln\left(1 + 6 \cdot \varepsilon \cdot x_0\right)} \qquad (3)$$

However, H_3PO_4-doped PBI membranes have an electro-osmotic drag coefficient that is almost negligible[30], so that the limiting current density can be considered as equal to the crossover one.

Figure 2

The lifetime test was performed galvanostatically at a fixed current density of 100 mA/cm^2. This is a typical value drawn under real operating conditions for a cell[49]. Measurements were started in the morning and interrupted at night, with the methanol solution renewed every day during the 10 days of operation. The cell was fixed at a temperature of 175 ºC. The fuel was a methanol/water mixture with a wt. ratio of 0.5. This solution was kept at a temperature of 100 ºC. The next day the cell was again heated up to 175 ºC.

3. Results and discussion

3.1. Influence of the temperature on the cell performance

The influence of the temperature (125–150–175–200 ºC) on the cell voltage (a), the power output (b), and each electrode potential (c) is represented in Figure 3. The variation of the OCV and crossover currents for the four different temperatures are shown in Figure 3(d). The cell was operated with pure oxygen at atmospheric pressure. The methanol/water wt. ratio was 0.5.

Figure 3

Inspection of Figure 3(a) shows that an increase in the cell performance occurs as the temperature increases. Thus, at 0.1 A cm^{-2}, the cell voltage was 270 mV at 125 ºC, 310 mV at 150 ºC, 395 mV at 175 ºC and 473 mV at 200 ºC. The increase in the

performance with temperature can be explained in terms of the enhancement of the electrode kinetics and the decrease in the membrane resistance. This is reflected in the power output curves. Power peaks are 33.5 mW cm^{-2} at 125 ºC, 49.7 mW cm^{-2} at 150 ºC, 80 mW cm^{-2} at 175 ºC and 138.5 mW cm^{-2} at 200 ºC. The process occurring in the system is represented in Figure 3(c). Both the anode and cathode performances increase with temperature. The higher the temperature, the better the kinetics of the methanol oxidation and oxygen reduction processes. The marked enhancement of the cathodic process with temperature is quite significant. Apart from the aforementioned intrinsic enhancement in the kinetics, extensively shown for PBI-based systems[50-53], a higher tolerance of the cathode to methanol (faster oxidation), despite the increase in the methanol crossover current, could also account for this observation.

The change in the methanol crossover current and OCV is shown in Figure 3(d). One of the major reasons for the decrease in the OCV in a DMFC is methanol crossing the membrane. This methanol is directly oxidized in the cathode compartment, lowering its voltage and consuming a proportion of the combutent[54]. Therefore, the open circuit voltage is an indirect measurement of the methanol crossover effects[55]. It can be seen that the OCV increases as the temperature increases, thus confirming the less detrimental effects of methanol crossover at the highest temperatures. This situation was also observed[54-56] for perfluorinated systems, where the methanol permeation is more marked (e.g., a methanol crossover current of 70 mA cm^{-2} was measured for a Nafion® 117 membrane with a 1 M MeOH solution, compared to PBI, whose crossover current is 15 mA cm^{-2} for an equivalent methanol concentration of ≈ 14 M, which is close to that reported by Wang et al.[26]).

The PBI crossover current increases with temperature. However, the increase becomes less marked as the temperature increases. The reasons for this behavior are not clear. It is possible that some membrane dehydration takes place at the highest temperatures, leading to the formation of some pyrophosphoric acid. The presence of this species might make the membrane less permeable to methanol, thus offsetting the effect of the temperature. Indeed, Liu et al.[57] reported a decrease in the gas solubility of PBI as their system became drier. Further studies must be carried out to understand this behavior. Notwithstanding, this particular behavior may explain the rather notable increase in the cathodic (and overall) performance between 175 and 200 ºC compared to the other systems, as well as the intrinsic effect of the temperature upon the kinetic of the oxygen reduction reaction and the electrolyte conductivity.

3.2. Influence of the methanol concentration on the cell performance

The influence of the methanol concentration on the cell voltage (a), the power output (b), and each electrode potential (c) is shown in Figure 4. Four methanol/water (*M*/*W*) wt. ratios (molar ratio in brackets) were studied, 0.25 (0.14), 0.5 (0.28), 1 (0.56) and 2 (1.12). The variation of the OCV and crossover currents with the M/W ratio are shown in Figure 4(d).

Figure 4

The cell performance at the four methanol concentrations studied is represented in Figure 4(a). It is quite interesting to consider the particular behavior of the system, especially at low and high current density. At low current density, which is the region of activation polarization where the kinetics of the electrochemical processes govern the performance, the cell has better performance with larger amounts of water. The

catalytic layer is formed by the catalyst itself and a certain amount of electrolyte in order to provide a pathway for the protons. As a consequence, in order to obtain a highly active catalyst, an electrolyte with a high conductivity is desirable and this is achieved with the highest water content. In this situation the three-phase interface necessary for the reaction is maximized, thus improving the cell performance. At high current density, where the mass transfer processes dominates the performance, the best performance is achieved for the intermediate M/W ratio of 0.5. A lower M/W value reduces the cell performance in this region – probably due to the reduced availability of methanol. M/W values of 1 and 2 gives rise to worse performance. An increase in the methanol vapor pressure is detrimental and leads to an increase in the methanol crossover [see Figure 4(d)]. Moreover, Lin et al.[34] reported that low water availability reduces the tendency to form OH species, which are crucial for complete methanol oxidation. Indeed, they stated that above an M/W ratio of 0.89 (M/W molar ratio of 0.5), a proportion of the methanol feed is not completely oxidized. This may reduce the efficiency of the system and the cell performance overall. In addition, a low water content reduces the PBI conductivity, which could also contribute to the decrease in the performance.

The existence of an apparent optimum M/W is reflected in the maximum power peaks, 66.7 mW cm^{-2} at M/W = 0.25, 80 mW cm^{-2} at M/W = 0.5, 74.4 mW cm^{-2} at M/W = 1, and 61.9 mW cm^{-2} at M/W = 2. The potential of each electrode is shown in Figure 4(c) and this helps us to understand the cell results further. In the case of the anode, as in the case of the overall performance, a high water content is beneficial except at high current density, where a large amount of methanol is required. This explains the significant increase in potential at an M/W of 0.25. A high methanol

concentration also impairs the anodic performance, a finding explained by the low water availability, which reduces the efficiency of the methanol oxidation and diminishes the electrolyte conductivity. In the case of the cathode, there is a steady increase in performance as the methanol concentration decreases. The drop in the methanol crossover accounts for this change. Nevertheless, despite the improvements in the cathodic performance, the overall performance decays at low M/W values, thus demonstrating the significant influence of the anodic process on the overall cell performance.

The change in the OCV and in the methanol crossover currents are represented in Figure 4(d). A decrease in the OCV is observed as the methanol concentration increases. The higher methanol permeation rate explains this drop, which is the result of a higher mixed potential effect. The crossover current increases with the methanol concentration, as expected from the higher methanol partial pressure in the anode compartment. However, interestingly, the increase is not linear. The higher the methanol concentration, the smaller the increase. Measurements of the methanol permeability in diffusion cells[27] have shown that the methanol permeability reaches a maximum at a certain concentration (around 50% vol.) and then decreases above this value. A clear explanation for this behavior has not been given, but it has been proposed that the possible formation of hydrogen bonds between the polymer and the methanol somehow blocks the passage of methanol. However, these measurements were performed on non-doped PBI and liquid methanol solutions, which are very different to the conditions used in our investigation. Though this could be a valid hypothesis to explain the observed behavior, a possible dehydration phenomenon that leads to the formation of pyrophosphoric acid can not be ruled out. As mentioned

previously, this larger species may reduce the methanol permeation. Further studies must be undertaken in order to analyze this particular behavior.

3.3. Combined effect of the temperature and the methanol concentration

In the previous sections, the effect of the temperature or the methanol concentration has been discussed under particular conditions. In this section, a complete study of the combined effect of these two parameters is described. All of the combinations of the four temperatures and methanol concentrations were analyzed. This study led to a large number of experimental polarization curves, with the cell voltage and each electrode performance investigated. It was considered that a good way to evaluate both effects together (temperature and methanol concentration) would be to represent the power peaks, which provide an idea of the actual performance. Besides, the OCV and the crossover currents provide information about the crossover process and its effects. The corresponding measurements are represented in Figure 5.

Figure 5

The power peaks for the cell are presented in Figure 5(a). The maximum power peak was attained with the cell operating at 200 ºC with a M/W ratio of 0.5. Moreover, it can be seen that, for the four different temperatures studied in this work, the optimum M/W is also 0.5. A detailed analysis of the decrease in the performance with temperature when the methanol concentration increases from 0.5 to 2 shows that the value at M/W = 2 is 43% of that at 0.5 at 200 ºC, 74% at 175 ºC, 80% at 150 ºC and 84% at 125 ºC. Low water availability is detrimental in terms of the kinetics of the methanol oxidation process and methanol crossover. A high temperature enhances these phenomena and is also associated with the possible start of electrolyte

dehydration. As expected, the lowest methanol concentration reduces the cell performance due to the low fuel availability. For a given methanol concentration, the analysis of the change in the performance is also interesting. In all cases, it can be seen that a higher performance is obtained at higher temperature, except for an M/W of 2. In that case, the performance decreases between 175 and 200 ºC. In fact, a detailed analysis shows that the increase with temperature becomes less marked as the M/W increases. At 175 ºC the value of the power peak is 65% that at a M/W ratio of 0.25, 71% at 0.5 and 76% at 1, with respect to the power peak at 200 ºC. At a M/W ratio of 2, the power peak at 200 ºC is 97% of that at 175 ºC. This represents another way to observe the detrimental effect of the combination of a high methanol partial pressure and temperature in terms of overall performance.

Comparison of our results with other values reported in literature for PBI-based DMFC systems (including blends) and other high temperature DMFC systems would be interesting. However, such a comparison must be treated with caution, since the physico-chemical and electrochemical characteristics of the membranes in some cases are different and, furthermore, different kinds of catalysts (supported and unsupported) and noble metal loadings are used, as well as different pressures and temperatures. The values determined for some examples are collected in Table 1.

Table 1

It can be seen that the performance obtained in this work compares favorably with other PBI-based systems and high temperature DMFC cells, despite the differences in the operating conditions, catalyst loadings and materials. A reasonably low catalyst loading and backpressure gives rise to good performance, which may be due to a more

optimum distribution of the catalytic layer, maximizing the electrodic activity. Also, PBI appears to be a suitable material for operating a DMFC at high temperatures. This is due to its high conductivity compared to the other high temperature materials (inorganic composites of Nafion®), which allows us to exploit the expected enhancement in the kinetics. Likewise, PBI is very well positioned in terms of its blends, which in some cases can not operate above 100 ºC (Nafion®-PBI mixtures) or, if they can, require hydration because of the other components. This requirement limits the operating temperature to 130 ºC.

The change in the OCV and crossover currents with the methanol concentration and temperature are shown in Figures 5(b) and 5(c). In the case of the OCV, it can be seen that this always decreases with the M/W ratio due to the higher methanol permeation rate. An increase in the OCV for the four methanol concentrations can be seen as the temperature increases. This increase shows the higher tolerance of the cathode to the methanol crossover, since methanol can be more rapidly oxidized in the cathode. The crossover currents show the expected trend of increasing with temperature and M/W. However, for the combination of an increase in the temperature and the M/W the increase is not linear. The reasons for this particular characteristic of PBI membranes were described in the previous sections.

3.4. Influence of the oxygen partial pressure

In order to study the influence of the oxygen partial pressure on the cell performance, two types of studies were carried out. In the first study, the results of which are shown in Figure 6, the influence of the replacement of oxygen by air was studied. In the

second study, the influence of pressurizing the cathode with 1 bar (relative) was investigated and the results are represented in Figure 7. Two methanol/water wt. ratios were used (0.5 and 1). In the case of the measurements with the same M/W, the anodic curves (not shown) were equal. In addition, the two M/W values were intentionally chosen since their anodic curves are similar [Figure 4(c)], meaning that the differences in the cell performance are related to the cathodic performance alone. The temperature for the measurements represented in Figures 6 and 7 was 175 ºC.

The effect of replacing oxygen with air on the cell voltage and power output is shown in Figure 6. Firstly, the classical effect of reducing the oxygen partial pressure can be observed. For example, at 0.1 A cm^{-2}, for a M/W ratio of 0.5, the cell voltage with O_2 is 395 mV whereas it is 297 mV for air. For a M/W ratio of 1, the corresponding voltages are 386 mV and 240 mV for oxygen and air, respectively. This change is also reflected in the power peaks. For M/W ratio of 0.5, the corresponding peaks are 74.8 mW cm^{-2} for O_2 and 37.9 mW cm^{-2} for air. In the case of the M/W of 1, the peaks are 69.8 mW cm^{-2} for O_2 and 25.5 mW cm^{-2} for air. The increase in the partial pressure of the reactant, the higher solubility of the gas and the better mass transfer rate explain this observation. However, it is worth noting that the decrease is greater for the M/W of 1 than for 0.5. Taking into account that the anodic performances are very similar, the differences must arise from the different cathodic performance. Ge et al.[64] observed similar behavior with a Nafion® membrane when they studied the influence of replacing the comburent at different methanol concentrations. A higher methanol concentration is associated with a higher permeation rate. When the methanol reaches the cathode, it is directly oxidized to CO_2 and H_2O, consuming a proportion of the O_2 that arrives in the catalyst layer. This reduces the O_2 availability and also creates a

mixed potential and poisons the catalyst. The higher the level of methanol permeation, the more noticeable these phenomena become. On using air, the methanol permeation effects become even more important, as demonstrated by the results obtained.

Figure 6

The effect of pressurizing the cathode is shown in Figure 7. The measurements were carried out using air as the comburent. In a similar way to the replacement of air by oxygen, pressurizing the cathode also increases the cell performance. At a current density of 0.1 A cm^{-2}, the cell voltage for a M/W ratio of 0.5 is 297 mV without cathode backpressure and 360 mV with 1 bar of backpressure. For the M/W of 1, in the absence of back pressure the voltage was 240 mV and at 1 bar the value was 339 mV. The corresponding power peaks are as follows; for the M/W ratio of 0.5 the values are 37.9 mW cm^{-2} for air without backpressure and 52 mW cm^{-2} for air at 1 bar. For a M/W ratio of 1, the power peaks are 25.5 mW cm^{-2} for air without backpressure and 46 mW cm^{-2} for air at 1 bar. The observed enhancement is due to the increase in the partial pressure of reactants, the higher solubility of the gas and the better mass transfer rate.

Figure 7

When the air is replaced by oxygen, the oxygen partial pressure increases by a factor of five, whereas it increases by a factor of two when the system is pressurized to 1 bar. This change gives rise to greater increases in the power peaks in the case where O_2 is used (average of 2.2) compared to the pressurization with air (average of 1.4), but this increase is not concomitant with the increases in the partial pressure. More marked improvements might be expected on using O_2 compared to the effect of

doubling the oxygen partial pressure. It is possible that when pressure is not applied, some parts of the electrode (edges) may be gas-tight and therefore practically inactive, especially in small electrodes[65]. This would be expected to diminish the effect of the increase in the oxygen partial pressure on replacement of air by oxygen.

In order to gain a better insight into the combined effects of the oxygen partial pressure, methanol concentration and temperature, the power peaks for the cell performance at two different levels of these operating parameters are given in Table 2. The corresponding OCV data are presented in Table 3. If we consider the power peaks, the trends are the same as those described above. The lower the oxidant partial pressure and the temperature, the greater the decrease in the power peak when a higher M/W ratio is used. The value of the power peak with M/W = 1 at 175 ºC with air is 67.3% of that at M/W = 0.5 under the same conditions. The value on pressurizing the system at 1 bar is 88.5%. At 200 ºC, with no backpressure and with air, the percentage is 71.8%. With oxygen at 175 ºC and no backpressure, the value is 93.3%. The increase in the performance observed on using a pressurized system due to the replacement of air by O_2 is more marked. Upon pressurization, oxygen can also be forced into the stagnant regions, which are now able to produce current, reflecting more realistically the effect of the comburent substitution. Thus, when backpressure is not used, at 175 ºC and with a M/W ratio of 0.5, the value obtained on using O_2 is 97% higher. With 1 bar of back pressure, the increase is 142%. The same trends are found for the other pairs of conditions, regardless of the temperature and methanol concentration. Moreover, the values shown in Table 2 also follow the trend described in the previous paragraph.

Table 1

The OCV values shown in Table 3 were obtained under the same conditions as those in Table 2. An increase in the temperature increases the OCV as a result of the higher tolerance of the cathode to methanol and the faster kinetics of its oxidation. Independently of the temperature, an increase in M/W reduces the OCV due to the more prominent crossover effects. It can also be seen how the OCV increases with the O_2 usage or when the system is pressurized, revealing that the higher comburent availability reduces the mixed potential. As expected, the changes in the OCV are smaller at 200 ºC than at 175 ºC and when the system is pressurized. Other typical trends in behavior, similar to those already described above, can also be observed from the results in Table 2.

Table 2

3.5. Durability test

The results of a durability test performed intermittently on the cell during 10 days operating for 12 hours are shown in Figure 8. The experiments were performed with oxygen at 175 ºC, with a M/W ratio of 0.5. The applied load was 100 mA cm^{-2}.

Figure 8

Firstly, it can be seen how the cell performance is rather stable over the 10 days of the experiment. This result is very satisfactory and promising, since this type of measurement, to the best of our knowledge, has never been carried out for this type of vapor-fed pure PBI-based DMFC. If we consider the curves obtained for each day, it can be seen how they follow a similar pattern. There is an initial decrease in the cell voltage and this is followed by a voltage increase. The initial decrease observed each day can be explained as follows. The protocol for this measurement stipulated that the

cell should be stopped overnight. However, the temperature was kept at 100 ºC in order to avoid condensation of the fuel or the water produced in the cathode, which may wash out the H_3PO_4. This could allow the remaining vapor fuel mixture or vapor in the cathode to be expelled. Therefore, the next day the system is "free" of methanol. The initial data are taken at the beginning of the experiment. At that moment, the detrimental methanol crossover effect might not be fully developed. The voltage then abruptly decreases during the initial moments of the experiment before slowly starting to recover. Hence, the initial poisoning of the cathode catalyst by the methanol permeating the membrane may explain that decay. Chen et al.[66] also observed a decrease in the cell performance at the beginning of a durability test, attributing it to a possible non-equilibrium between ruthenium oxides in the anode catalyst. This phenomenon could also have taken place in the system described here. After the initial drop, the performance increased slightly or remained constant at around 395 mV. Hu et al.[67], for an H_2/O_2 PBI-based PEMFC, observed an analogous slight increase in the cell performance during the first hours of a lifetime test. They attributed this to an expansion of the three-phase zone where the electrochemical reaction occurs. Such a situation could also be applicable in our system. After the methanol crossover effects have been established, the system starts to activate and this increases its performance. The fact that this happens every day is quite significant and can be explained as follows. When the cell is "stopped", neither fuel mixture nor comburent is fed into the cell and no current is drawn. The cell is kept for 12 hours at 100 ºC and this could lead to some electrolyte dehydration. This element is very important in order to have an active electrocatalyst[68]. When the cell is restarted, a vapor methanol/water mixture is fed into the anode and water vapor is produced in the cathode. This rehydrates the electrolyte, increasing its conductivity and, as a

consequence, enhances the catalyst activity. Once the 12 hour measurement period has elapsed the cycle commences again.

In any case, as mentioned above, the most outstanding feature is that during those 10 days of operation the cell voltage hardly drops, indicating that the cell (and all its elements – catalyst, PBI membrane, gas diffusion support) behavior is relatively stable. Although this period is too short to extract any definitive conclusion, especially taking into account that much longer durability tests have been reported for H_2-fed PBI-based PEMFC[67,69-71], this result can be considered as very promising and encouraging. Future studies are of great interest in order to assess the stability of the system on a much longer time scale. The influence of some operating variables, such as the temperature, the use of air or O_2, flow of the fuel and comburent, fuel concentration, etc., on the cell operation is also of interest.

3.6. Comparison with Nafion®-based DMFC

In order to conclude this work, the performance between the most widely used membrane material in DMFC, Nafion®, and PBI was carried out. Although the operating conditions for each type of the cell are very different (state of the fuel, operating temperature, electrode architecture, etc.), we could at least rank the PBI-based DMFC with respect to Nafion®-based DMFC in terms, for example, methanol permeation and tolerable methanol concentrations that can be used. In order to achieve this goal, intermediate conditions were used. The temperature for the Nafion® system was 70 ºC, which is intermediate in the range 50–90 ºC, and 150 ºC for the PBI system, which is in the range 100–200 ºC. Several methanol concentrations

(expressed as molarity of the feed liquid solution) were tested in both systems and methanol crossover currents were measured.

The performance of the cells under different conditions is represented in Figure 9. The performance using a 1 M methanol solution is shown in Figure 9(a). This value is typically used for Nafion®-based DMFC[1]. Firstly, it can be seen how the OCV is significantly higher for the PBI system, 805 mV vs. 626 mV for the Nafion® system. At low current densities the performance is also higher for the PBI system compared to the Nafion® cell. However, at around 100 mA cm^{-2} the performance rapidly decreases, showing significant mass transfer limitations. This is not the case for the Nafion® system. The sudden decrease in performance can be explained in terms of the low methanol permeability in the PBI system. This is tremendously beneficial for a material as a membrane (low methanol crossover). However, PBI is also present in the electrode as a crucial element to maximize the three-phase interface[65]. When methanol reaches the catalyst, it has to go through the electrolyte that covers it in order to reach a catalytically active site. The low methanol permeability limits the access of the fuel to the active sites, thus reducing the performance when the system requires a high methanol concentration. In addition, the different state of the fuel (liquid in the Nafion® system and vapor in the PBI one) might account for these differences. The performance of the two systems when a 10 M methanol solution was used is compared in Figure 9(b). The performance of Nafion® is appreciably lower than that of PBI. The OCV is 419 mV for Nafion® and 591 mV for PBI. The massive methanol permeation in the Nafion® system explains its low performance. Indeed, the anode overvoltage (not shown) is only slightly higher than that obtained with 1 M MeOH, meaning that the cathode is the electrode that limits the performance. In the

case of PBI, a much higher performance can be attained since the previously observed mass transfer limitations are now overcome. The best performances achieved in both systems are represented in Figure 9(c). It can be observed that the performances are comparable, which confirms the PBI polymer as a good candidate for DMFC. It is important to point out that these results were obtained using electrodes without an optimum structure. Further performance improvements could be achieved, especially in the field of PBI-based DMFC, where little effort has been devoted to this area. Furthermore, this system exploits the benefit of working with high methanol concentrations, which can be considered advantageous in practical terms when using a DMFC in an actual application[44].

Figure 9

The change in the OCV and crossover currents for Nafion® (electro-osmotic coefficient drag of 3.2[32]) and PBI are shown in Figure 10. As expected, the crossover current increases with the methanol concentration, and the values for Nafion® are almost two orders of magnitude higher than those of PBI. However, the increase is much more notable for the Nafion® membrane. In the case of the OCV, for both systems, the crossover current decreases with the methanol concentration. Once again, Nafion® undergoes a more noticeable decrease, showing a more marked mixed potential that results from its larger methanol crossover compared to PBI. Indeed, when the methanol concentration exceeds 5 M, the OCV drops below 500 mV, whereas in the case of PBI the OCV almost reaches a plateau and does not decrease abruptly.

Figure 10

Finally, an interesting way of comparing the fuel cell performance is in terms of efficiency. Two ways have been proposed to assess this parameter: (i) energy efficiency, expressed in terms of mW h g^{-1}_{MeOH} cm^{-2}, from the quotient of the maximum power peak and the mass flow of methanol, and (ii) the efficiency (η_{DMFC}) as suggested by Silva et al.[2]. This latter approach takes into account the two main limiting factors in a DMFC, i.e. the poor kinetics of the methanol oxidation at the anode and the permeation of the methanol through the membrane. The following expression is used to calculate this parameter.

$$\eta_{DMFC} = \eta_E \eta_F \tag{3}$$

where η_E is the potential efficiency

$$\eta_E = {E_{cell}}/{E_{rev}} \tag{4}$$

where E_{cell} (mV) is the actual cell potential and E_{rev} (mV) is the reversible voltage of the DMFC.

The Faraday efficiency (η_F) is evaluated from:

$$\eta_F = \frac{j}{j + j_{cross}} \tag{5}$$

where j (mA cm^{-2}) is the current density drawn from the cell and j_{cross} (mA cm^{-2}) the equivalent current for the amount of methanol that crosses the membrane.

Both kinds of efficiencies change with the current density. In order to simplify matters, this comparison is made in terms of the maximum efficiency values. The

corresponding values for the conditions shown in Figures 9 and 10 are shown in Table 4.

Table 4

In terms of energy efficiency, Nafion® is more effective than PBI since its performance is higher with low methanol concentrations. When the methanol concentration increases, the energy efficiency evidently diminishes but in this case PBI is more efficient than Nafion® as the latter can not tolerate high methanol concentrations. In terms of the efficiency, which reflects the cell performance, and the methanol crossover, PBI outperforms Nafion®. This reflects the enhancement in the kinetic on increasing the temperature and the lower methanol crossover, as described in the previous paragraph.

4. Conclusions

The following conclusions can be drawn from this work:

- A PBI-based vapor-fed DMFC test system has been satisfactorily implemented and enabled a study into the influence of the temperature, methanol/water ratio and O_2 partial pressure on the cell performance.
- An increase in temperature improves the cell performance due to the enhancement in the kinetics of the electrode reactions and the electrolyte conductivity. In addition, and despite the increase in the crossover, the higher tolerance of the cathode to the methanol crossover also contributes to the increase in the performance.
- The fuel composition expressed in terms of methanol/water wt. ratio has an optimum value of 0.5. A lower amount of methanol promotes the appearance

of mass transfer limitations. The higher methanol crossover and lower water availability have a detrimental effect on cell performance at high methanol concentrations.

- An increase in the oxygen partial pressure improves the cell performance. This change facilitates access of the comburent to the catalyst sites. Moreover, the effects of the methanol crossover are reduced.
- The durability test showed quite stable performance (≈ 390 mV) over 120 hours of intermittent test at 100 mA cm^{-2}, which is considered to be a promising and encouraging result.
- The primary comparison with the traditional Nafion® membrane served to highlight PBI as an interesting candidate for DMFC. The low methanol permeability of this material and the chance of working at high temperature should attract attention to this non-fluorinated membrane.

Acknowledgements

This work was supported by the Ministry of Education and Science of the Spanish Government through project CTM2004, which includes a pre-doctoral grant awarded to J.J. Linares, and by the JCCM (Junta de Comunidades de Castilla-La Mancha, Spain) through the project PBI-08-0151-2045.

References

(1) Aricò, A.S.; Srinivasan, S.; Antonucci, V. *Fuel Cells* **2001**, 1, 133–161.

(2) Silva, V.S.; Weisshaar, S.; Reissner, R.; Ruffmann, B.; Vetter, S.; Mendes, A.; Madeira, L.M.; Nunes, S. *J. Power Sources* **2005**, 145, 485–494.

(3) Jörissen, L.; Gogel, V.; Kerres, J.; Garche, J. *J. Power Sources* **2002**, 105, 267–273.

(4) Peluca, N.W.; Elabd, Y.A. *J. Polym. Sci.: Part B: Polym. Phys.* **2006**, 44, 2201–2225.

(5) Scott, K.; Taama, W.M.; Argyropoulos, P. *J. Power Sources* **1999**, 79, 43–59.

(6) Jha, N; Reddy, A.L.M.; Shaijumon, M.M.; Rajalakshmi, N.; Ramaprabhu, S. *Int. J. Hyd. Energy* **2008**, 33, 427–433.

(7) Neburchilov, V.; Wang, H.; Zhang, J. *Electrochem. Comm.* **2007**, 9, 1788–1792.

(8) Lo, M.-Y.; Liao, I-H.; Huang, C.-C. *Int. J. Hyd. Energy* **2007**, 32, 731–735.

(9) Shao, Z.-G.; Lin, W.-F.; Christensen, P.A.; Zhang, H. *Int. J. Hyd. Energy* **2006**, 31, 1914–1919.

(10) Papageorgopoulos, D.C.; Liu, F.; Conrad, O. *Electrochim. Acta* **2007**, 52, 4982–4986.

(11) Sun, G.Q.; Wang, J.T.; Savinell, R.F. *J. Appl. Electrochem.* **1998**, 28, 1087–1093.

(12) Yuan, W.; Scott, K.; Cheng, H. *J. Power Sources* **2006**, 163, 323–329.

(13) Manea, C.; Mulder, M. *Desalination* **2002**, 147, 179–182.

(14) Kerres, J.; Zhang, W.; Jörissen, L.; Gogel, V. *J. New Mat. Electrochem. Sys.* **2002**, 5, 97–107.

(15) Neburchilov, V.; Martin, J.; Wang, H.; Zhang, J. *J. Power Sources* **2007**, 169, 221–238.

(16) Shen, M.; Roy, S.; Kuhlmann, J.W.; Scott, K.; Lovell, K.; Horsfall, J.A. *J. Membr. Sci.* **2005**, 251, 121–130.

(17) Hogarth, M.; Christensen, P.; Hamnett, A.; Shukla, A. *J. Power Sources* **1997**, 69, 113–124.

(18) Hogarth, M.; Christensen, P.; Hamnett, A.; Shukla, A. *J. Power Sources* **1997**, 69, 125–136.

(19) Fukunaga, H.; Ishida, T.; Teranishi, N.; Arai, C.; Yamada, K. *Electrochim. Acta* **2004**, 49, 2123–2129.

(20) Kim, H. *J. Power Sources* **2006**, 162, 1232–1235.

(21) Guo, Z.; Faghri, A. *J. Power Sources* **2007**, 167, 378–390.

(22) Qingfeng, L.; Hjuler, H.A.; Bjerrum, N.J. *J. Appl. Electrochem.* **2001**, 31, 773–779.

(23) He, R.; Li, Q; Xiao, G.; Bjerrum, N.J. *J. Membr. Sci.* **2003**, 226, 169–184.

(24) Lobato, J.; Cañizares, P.; Rodrigo, M.A.; Linares, J.J.; Manjavacas, G. *J. Membr. Sci.* **2006**, 280, 351–362.

(25) Wainright, J.S.; Wang, J.-T.; Weng, D.; Savinell, R.F.; Litt, M. *J. Electrochem. Soc.* **1995**, 142, L121–L123.

(26) Wang, J.-T.; Wasmus, S.; Savinell, R.F. *J. Electrochem. Soc.* **1996**, 143, 1233–1239.

(27) Pu, H.; Liu, Q.; Liu, G. *J. Membr. Sci.* **2004**, 241, 169–175.

(28) Li, Q.; He, R.; Berg, R.W.; Hjuler, H.A.; Bjerrum, N.J. *Solid State Ionics* **2004**, 168, 177–185.

(29) He, R.; Li, Q.; Jensen, J.O.; Bjerrum, N.J. *J. Polym. Sci. Part A: Polym. Chem.* **2007**, 45, 2989–2997.

(30) Weng, D.; Wainright, J.S.; Landau, U.; Savinell, R.F. *J. Electrochem. Soc.* **1996**, 143, 1260–1263.

(31) Choi, K.-H.; Peck, D.-H.; Kim, C.S.; Shin, D.-R-; Lee, T.-H. *J. Power Sources* **2000**, 86, 197–201.

(32) Ren, X.; Springer, T.E.; Gottesfeld, S. *J. Electrochem. Soc.* **2000**, 147, 92–98.

(33) Wang, J.-T.; Wainright, J.S.; Savinell, R.F.; Litt, M. *J. Appl. Electrochem.* **1996**, 26, 751–756.

(34) Lin, W.-F.; Wang, J.-T.; Savinell, R.F. *J. Electrochem. Soc.* **1997**, 144, 1917–1922.

(35) Sun, G.-Q.; Wang, J.-T.; Gupta, S.; Savinell, R.F. *J. Appl. Electrochem.* **2001**, 31, 1025–1031.

(36) Wang, J.; Wasmus, S.; Savinell, R.F. *J. Electrochem. Soc.* **1995**, 142, 4218–4224.

(37) Wang, J.T.; Lin, W.F.; Weber, M.; Wasmus, S.; Savinell, R.F. *Electrochim. Acta* **1998**, 43, 3821–3828.

(38) Weber, M.; Wang, J.-T.; Wasmus, S.; Savinell, R.F. *J. Electrochem. Soc.* **1996**, 143, L158–L160.

(39) Hobson, L.J.; Nakano, Y.; Ozu, H.; Hayase, S. *J. Power Sources* **2002**, 104, 79–84.

(40) Wycisk, R.; Chisholm, J.; Lee, J.; Lin, J.; Pintauro, P.N. *J. Power Sources* **2006**, 163, 9–17.

(41) Ainla, A.; Brandell, D. *Solid State Ionics* **2007**, 178, 581–585.

(42) Silva, V.S.; Ruffmann, B.; Vetter, S.; Mendes, A.; Madeira, L.M.; Nunes, S.P. *Catal. Today* **2005**, 104, 205–212.

(43) Sukumar, P.R.; Wu, W.; Markova, D.; Ünsal, O.; Klapper, M.; Müllen, K. *Macrom. Chem.& Phys.* **2007**, 208, 2258–2267.

(44) Gubler, L.; Kramer, D.; Belack, J.; Ünsal, O.; Schmidt, T.J.; Sherer, G.G. *J. Electrochem. Soc.* **2007**, 154, 981–987.

(45) Lobato, J.; Cañizares, P.; Rodrigo, M.A.; Linares, J.J.; Aguilar, J.A. *J. Membr. Sci.* **2007**, 306, 47–55.

(46) http://www.goodfellow.com/csp/active/gfHome.csp

(47) Barton, S.C.; Patterson, T.; Wang, E.; Fuller, T.F.; West, A.C. *J. Power Sources* **2001**, 96, 329–336.

(48) Argyropoulos P.; Scott K.; Shukla A.K.; Jackson C. *J. Power Sources* **2003**, 123, 190–199.

(49) Shukla, A.K.; Jackson, C.L.; Scott, K.; Raman, R.K. *Electrochim. Acta* **2002**, 47, 3401–3407.

(50) Zhang, J.; Tang, Y.; Song, C.; Zhang, J. *J. Power Sources* **2007**, 172, 163–171.

(51) Kongstein, O.E.; Berning, T.; Børresen, B.; Seland, F.; Tunold, R. *Energy* **2007**, 32, 418–422.

(52) Lobato, J.; Cañizares, P.; Rodrigo, M.A.; Linares, J.J. *Electrochim. Acta* **2007**, 52, 3910–3920.

(53) Seland, F.; Berning, T.; Børresen, B.; Tunold, R. *J. Power Sources* **2006**, 160, 27–36.

(54) Jung, D.H.; Lee, C.H.; Kim, C.S.; Shin, D.R. *J. Power Sources* **1998**, 71, 169–173.

(55) Nakagawa, N.; Xiu, Y. *J. Power Sources* **2003**, 118, 248–255.

(56) Lobato, J.; Cañizares, P.; Rodrigo, M.A.; Linares, J.J.; Fernández-Fragua, A. *Chem. Eng. Sci*. **2006**, 61, 4773–4782.

(57) Liu, Z.; Wainright, J.S.; Savinell, R.F. *Chem. Eng. Sci.* **2004**, 59, 4833–4838.

(58) Aricò, A.S.; Antonucci, P.L.; Modica, E.; Baglio, V.; Kim, H.; Antonucci, V. *Electrochim. Acta* **2002**, 47, 3723–3732.

(59) Antonucci, P.L.; Aricò, A.S.; Cretì, P.; Ramunni, E.; Antonucci, V. *Solid State Ionics* **1999**, 125, 431–437.

(60) Lufrano, F.; Baglio, V.; Staiti, P.; Aricò, A.S.; Antonucci, V. *J. Power Sources* **2008**, 179, 34–41.

(61) Kim, H.-J.; Shul, Y.-G.; Han, H. *J. Power Sources* **2006**, 158, 137–142.

(62) Ren, S.; Sun, G.; Li, C.; Song, S.; Xin, Q.; Yang, X. *J. Power Sources* **2006**, 157, 724–726.

(63) Jones, D.J.; Rozière, J.; Marrony, M.; Lamy, C.; Coutanceau, C.; Léger, J.-M.; Hutchinson, H.; Dupont, M. *Fuel Cells Bulletin* **2005**, October 2005, 12–15.

(64) Ge, J.; Liu, H. *J. Power Sources* **2005**, 142, 56–69.

(65) Mennola, T. *Licentiate's thesis* Helsinki University of Technology **2000**.

(66) Chen, W.; Sun, G.; Guo, J.; Zhao, X.; Yan, S.; Tian J.; Tang, S.; Zhou, Z.; Xin, Q. *Electrochim. Acta* **2006**, 51, 2391–2399.

(67) Hu, J.; Zhang, H.; Zhai, Y.; Liu, G.; Yi, B. *Int. J. Hyd. Energy* **2006**, 31, 1855–1862.

(68) Costamagna, P.; Srinivasan, S. *J. Power Sources* **2001**, 102, 242–252.

(69) Li, Q.; He, R.; Jensen, J.O.; Bjerrum, N.J. *Fuel Cells* **2004**, 4, 147–159.

(70) Xiao, L.; Zhang, H.; Scanlon, E.; Ramanathan, L. S.; Choe, E.-W.; Rogers, D.; Apple, T.; Benicewicz, B.C. *Chem. Mater.* **2005**, 17, 5328–5333.

(71) Schmidt, T.J.; Baurmeister, J. *J. Power Sources* **2008**, 176, 428–434.

FIGURES AND TABLES

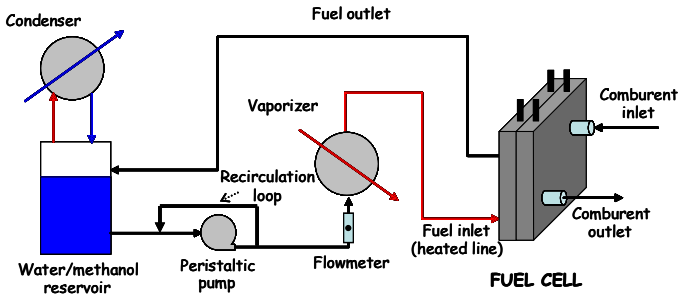

(a)

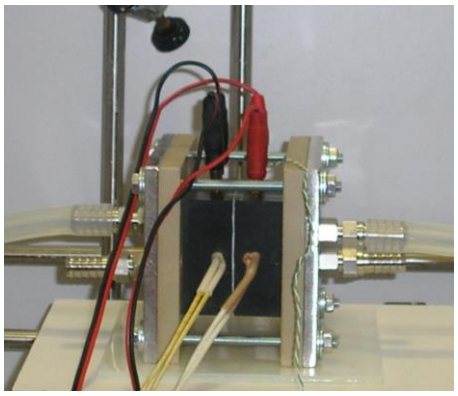

(b)

Figure 1. (a) Scheme of the experimental set-up; (b) Picture of the fuel cell

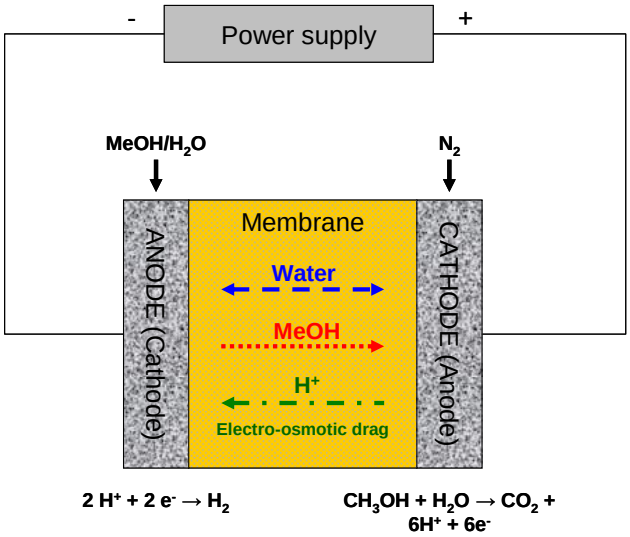

Figure 2. Representation of the methanol permeation measurement in the actual DMFC (the polarity of the electrodes in the permeation cell mode is indicated in brackets).

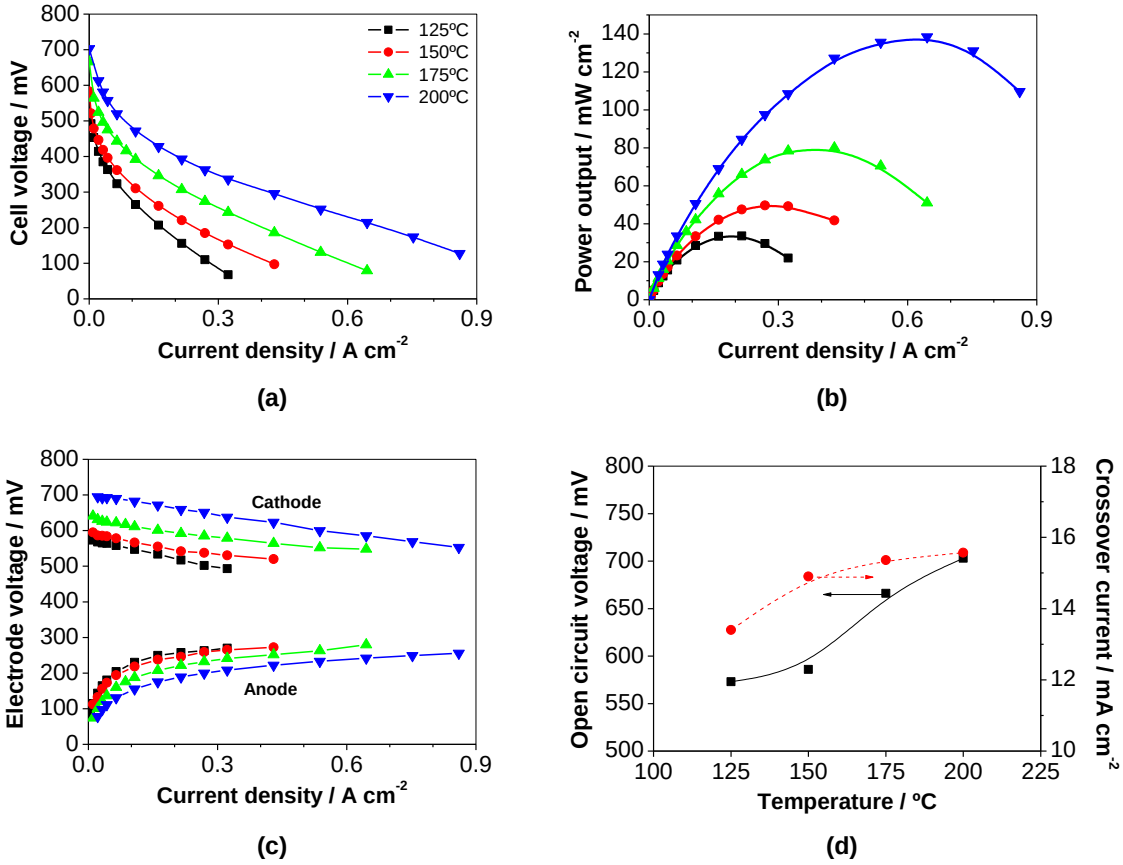

Figure 3. Influence of the temperature on the cell performance of a vapor-fed PBI-based DMFC (M/W = 0.5; cathode = pure O_2; no backpressure). (a) Cell voltage; (b) Power output; (c) Electrode overvoltage; (d) Open circuit voltage and methanol crossover current.

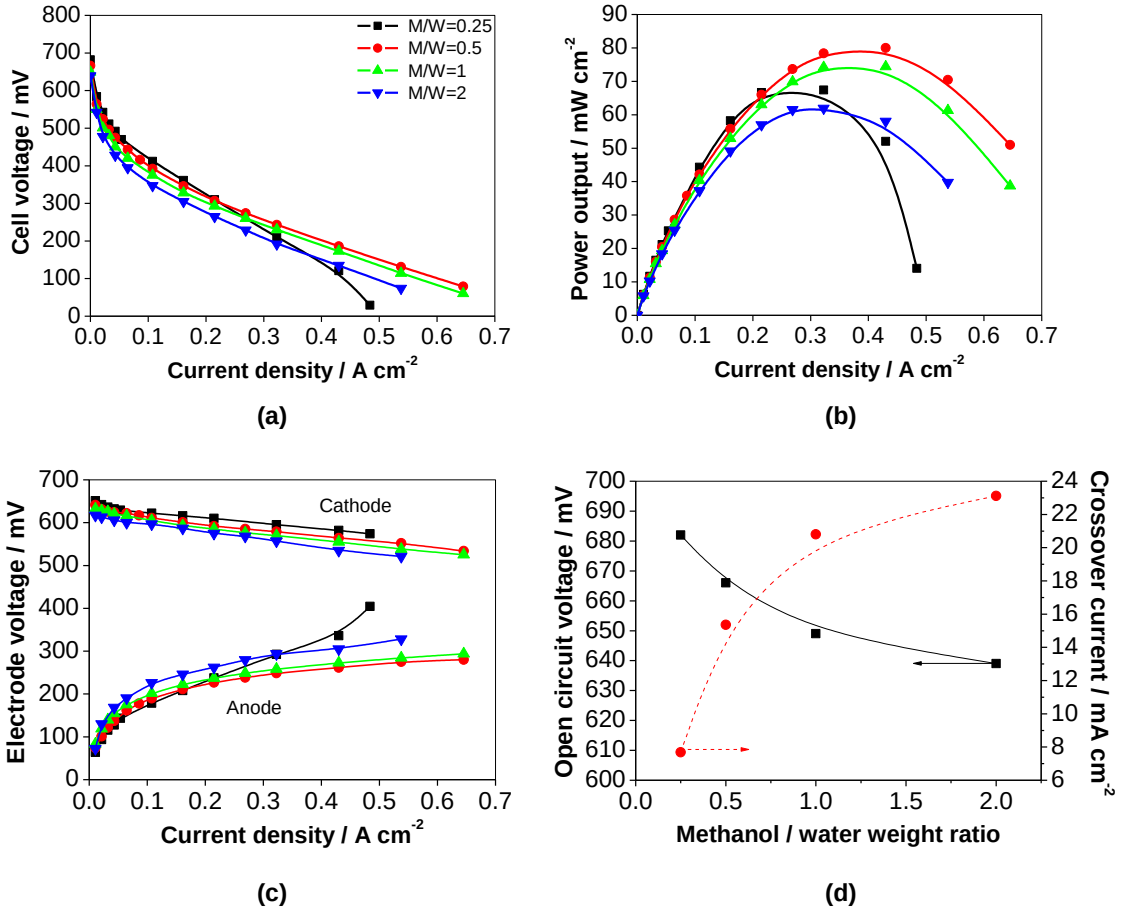

Figure 4. Influence of the methanol/water wt. ratio on the cell performance of a vapor-fed PBI-based DMFC (T = 175 ºC; cathode = pure O_2; no backpressure). (a) Cell voltage; (b) Power output; (c) Electrode overvoltage; (d) Open circuit voltage and methanol crossover current.

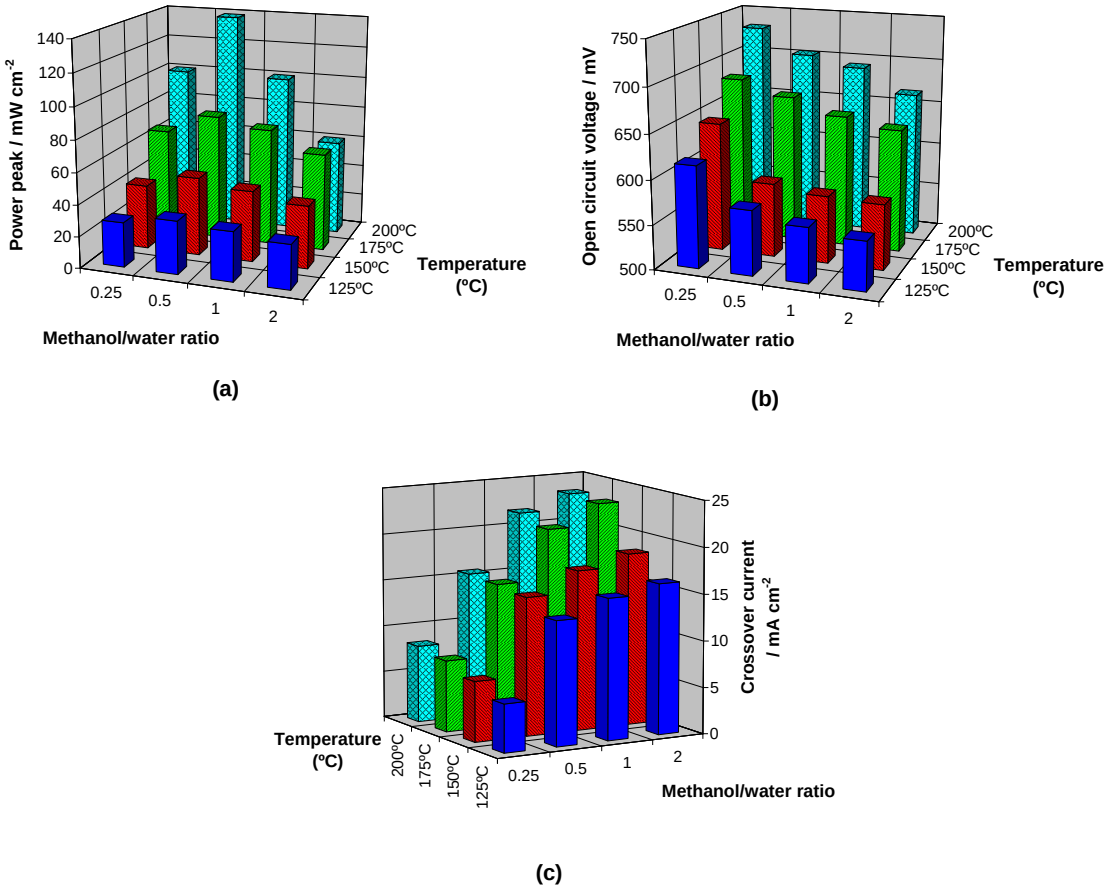

Figure 5. Combined influence of the temperature and methanol/water wt. ratio on the: (a) Power peaks; (b) Open circuit voltage; (c) Methanol crossover current.

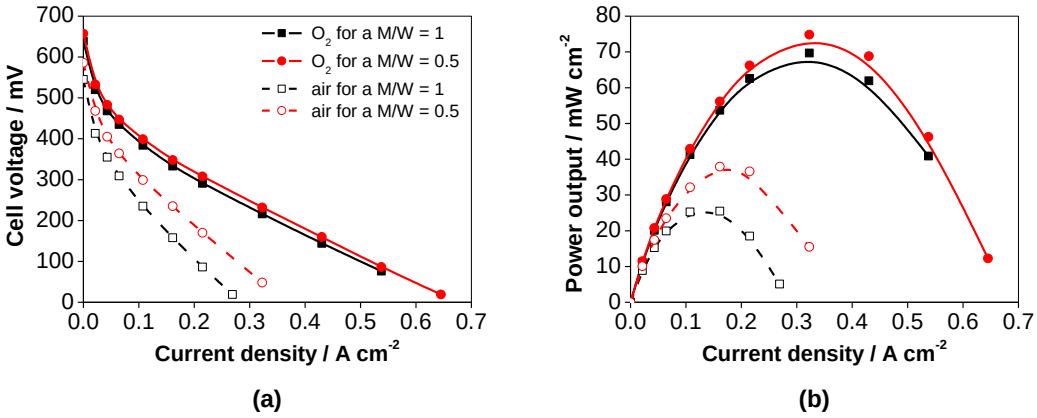

Figure 6. Influence of the comburent on the cell performance of a vapor-fed PBI-based DMFC (T = 175 ºC; no backpressure). (a) Cell voltage; (b) Power output.

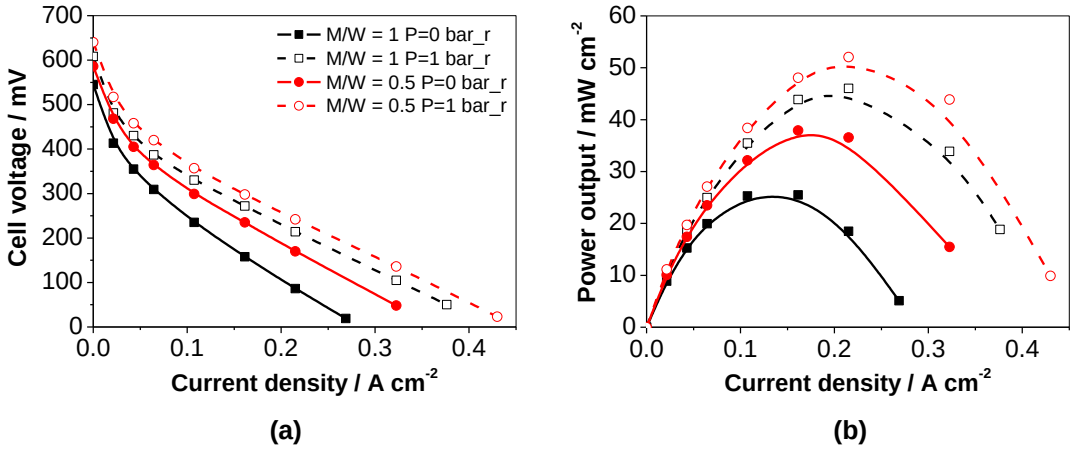

Figure 7. Influence of the comburent pressure on the cell performance of a vapor-fed PBI-based DMFC (T = 175 ºC; M/W = 0.5; cathode = air). (a) Cell voltage; (b) Power output.

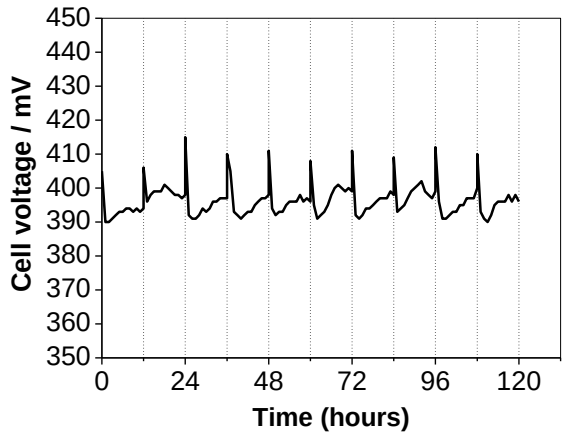

Figure 8. Evolution of the cell voltage during the intermittent durability test (10 days for 12 hours at 100 mA cm^{-2}; T = 175 ºC; M/W = 0.5; cathode = pure O_2; CH_3OH/O_2 = 1/1 atm). Running hours only are depicted. Dashed lines represent the overnight breaks.

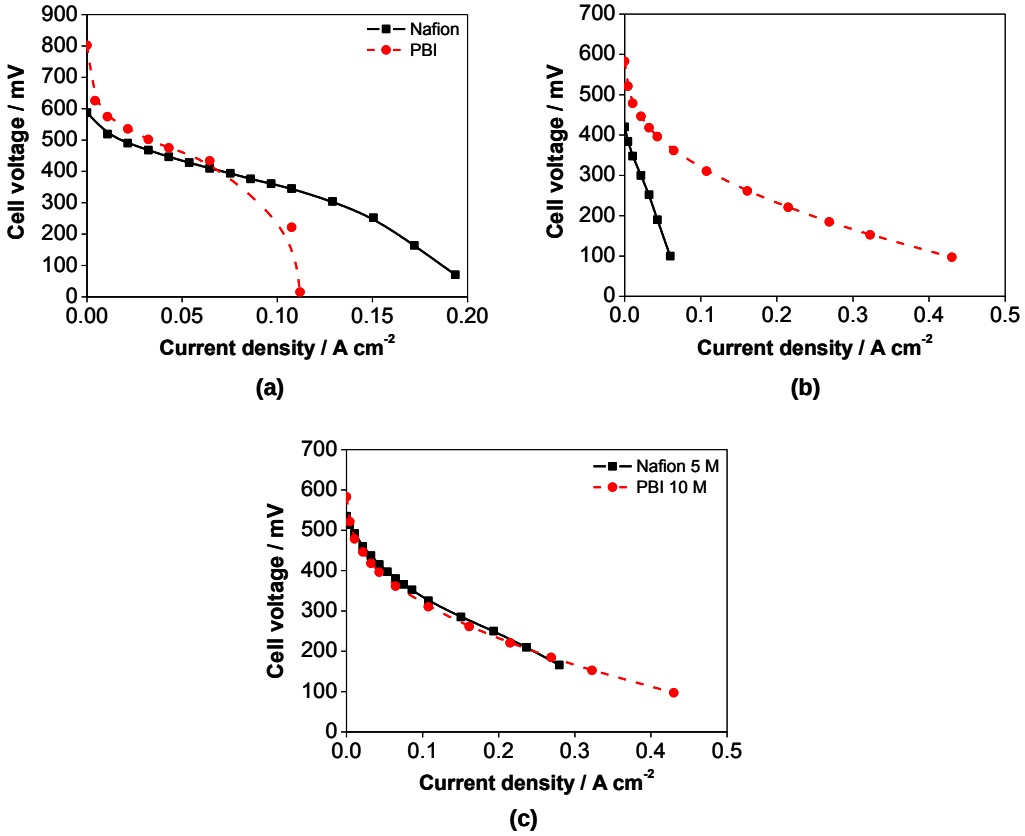

Figure 9. Comparison between the performances of a PBI-based and a Nafion®-based DMFC for: (a) methanol concentration = 1 M; (b) methanol concentration = 10 M; (c) under the conditions in which the maximum power is drawn from the system. (Cathode = pure O_2; CH_3OH/O_2 = 1/1 atm; T_{PBI} = 150 ºC; T_{Nafion} = 70 ºC).

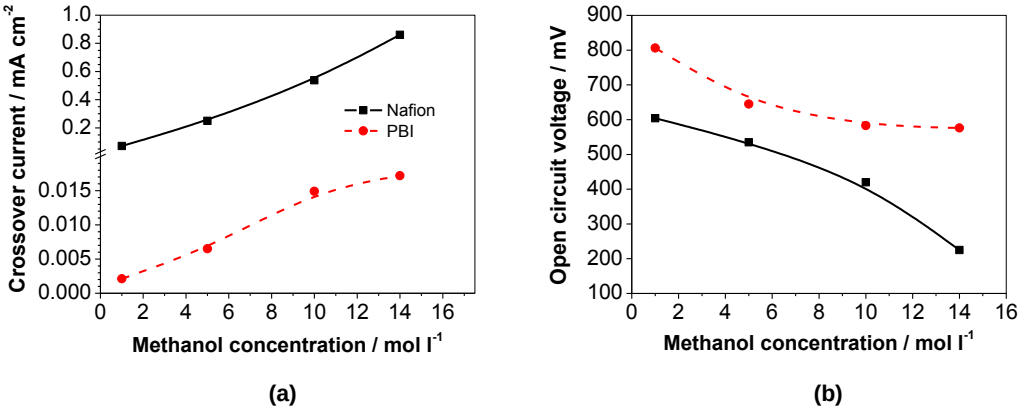

Figure 10. Comparison between a PBI-based and a Nafion®-based DMFC for: (a) crossover currents; (b) open circuit voltage. (T_{PBI} = 150 ºC; T_{Nafion} = 70 ºC)

Table 1. Comparison between the power peaks of different PBI-based DMFC systems and other high temperature systems.

Work	Catalyst loading / mg cm^{-2}		Fuel/ pressure†	Comburent/ pressure†	Membrane/ Temperature	Power peak / mW cm^{-2}
	Anode	Cathode				
This work	1 (PtRu/C‡)	1 (Pt/C)	M/W wt. ratio 0.5	O_2	H_3PO_4 doped PBI / 200 ºC	138.5
Wainright et al.[25] & Wang et al.[33]	4 (PtRu)	4 (Pt)	M/W molar ratio 4	O_2	H_3PO_4 doped PBI / 200 ºC	125
Gubler et al.[44]	1.5 (PtRu/C)	1 (Pt)	2 M MeOH / 3 bar	Air	Celtec V (PBI-PVPA) / 110 ºC	130
Wycisk et al.[40]	3 (PtRu/C)	4 (Pt/C)	1 M MeOH	Air	Nafion®-PBI / 60 ºC	100
Silva et al.[2]	1 (PtRu/C)	0.4 (Pt)	1.5 M MeOH / 2.5 bar	O_2 / 3 bar	sPEEK-ZrPh-PBI / 130 ºC	50.1
Hobson et al.[39]	n.a.	n.a.	2 M MeOH	Air	Nafion® 117 dipped in a PBI solution / 60 ºC	21.7
Jörissen et al.[3]	5 (PtRu)	6 (Pt)	1 M MeOH / 2.5 bar	Air / 4 bar	PEK-PBI-bPSU / 110 ºC	200
Kerres et al.[14]	5 (PtRu)	6 (Pt)	1 M MeOH / 2.5 bar	Air / 4 bar	PEK-PBI-PSU / 110 ºC	250
Aricò et al.[58]	2 (PtRu)	2 (Pt/C)	2 M MeOH / 2.5 atm	O_2 / 3 atm	Nafion® 112 / 130 ºC	390
Antonucci et al.[59]	2 (PtRu/C)	2 (Pt/C)	2 M MeOH / 4.5 atm	O_2 / 5.5 atm	Composite Nafion®-silica / 145 ºC	240
Lufrano et al.[60]	2 (PtRu/C)	2 (Pt/C)	2 M MeOH / 2.5 atm	O_2 / 3.5 atm	SPSf-silica / 120 ºC	180
Kim et al.[61]	4 (PtRu/C)	4 (Pt/C)	4 M MeOH	O_2	Sulfonic-functionalized heteropolyacid-silica nanoparticles / 200 ºC	44
Ren et al.[62]	n.a.	n.a.	1 M MeOH	O_2	Sulfonated zirconia-Nafion® / 105 ºC	4
Jones et al.[63]	1.2 (PtRu/C)	1.2 (Pt/C)	1 M MeOH / 2 bar	O_2 / 3 bar	sPEEK-ZrPh / 150 ºC	180

PVPA: polyvinylphosphonic acid; sPEEK: sulfonated poly(etheretherketone); ZrPh: zirconium phosphate; PEK: poly(etherketone); PSU: polysulfone; †: if backpressure is applied; ‡: M/C: catalyst supported on carbon, M: unsupported catalyst; n.a.: not available

Table 2. Power peaks of the cell for different temperatures (175/200 ºC), methanol/water weight ratio, comburent pressure and purity

	Backpressure			
	0 bar		**1 bar**	
Methanol/ water ratio	**O_2**	**Air**	**O_2**	**Air**
0.5	74.8 / 132.4	37.9 / 61.2	125.9 / 222.2	52.0 / 80.5
1	69.8 / 118.1	25.5 / 43.8	125.6 / 220.9	46.0 / 72.5

Table 3. Open circuit voltage of the cell for different temperatures (175/200 ºC), methanol/water weight ratio, comburent pressure and purity

	Backpressure			
	0 bar		**1 bar**	
Methanol/water ratio	**O_2**	**Air**	**O_2**	**Air**
0.5	657 / 692	586 / 626	685 / 736	635 / 681
1	639 / 683	545 / 611	671 / 729	611 / 669

Table 4. Evaluation of the efficiency of the system for the Nafion® and PBI membranes

Membrane	**[CH_3OH] / mol l^{-1}**	**Energy efficiency / mW h g^{-1}_{MeOH} cm^{-2}**	**DMFC efficiency /%**
Nafion® 117	1	10.21	17.19
	5	2.59	9.03
	10	0.21	1.18
PBI	1	7.29	41.32
	10	1.29	24.93